A Promising Way To Enhance the Electrochemical Behavior of Flexible Single-Walled Carbon Nanotube/Polyaniline Composite Films

ARTICLE *in* THE JOURNAL OF PHYSICAL CHEMISTRY C · OCTOBER 2010

Impact Factor: 4.77 · DOI: 10.1021/jp1092042

3 AUTHORS, INCLUDING:

Jilei Liu
Nanyang Technological University
28 PUBLICATIONS **594** CITATIONS
SEE PROFILE

Jing Sun
Chinese Academy of Sciences
229 PUBLICATIONS **6,914** CITATIONS
SEE PROFILE

A Promising Way To Enhance the Electrochemical Behavior of Flexible Single-Walled Carbon Nanotube/Polyaniline Composite Films

Jilei Liu, Jing Sun,* and Lian Gao*

The State Key Lab of High Performance Ceramics and Superfine Microstructure, Shanghai Institute of Ceramics, Chinese Academy of Sciences, 1295 Ding Xi Road, Shanghai 200050, People's Republic of China

Received: July 29, 2010; Revised Manuscript Received: October 8, 2010

In this work, flexible single-walled carbon nanotube/polyaniline (SWNT/PANi) composite films have been synthesized through an in situ electrochemical polymerization/degradation process. In addition to their good flexibility and light weight, cyclic voltammetry (CV) tests revealed that free-standing SWNT/PANi composite films also showed good electrochemical properties. Before electrodegradation, the highest specific capacitance, 501.8 F/g, was obtained for SWNT/PANi composite films with 90 electrochemical polymerization cycles. It reached values up to 706.7 F/g after electrodegradation, an increase of ~40%, which was attributed to more available charge-transfer channels and increased polycrystalline PANi regions that were produced by the dissolution of off-lying disordered PANi.

Introduction

Electrochemical capacitors (ECs), which are also known as supercapacitors, are energy storage devices that combine some virtues of batteries and electric double layer capacitances (EDLCs), such as high power density, fast charge/discharge ability and long cycle life.[1−4] These unique advantages make them the most promising vehicles in various energy storage devices. Carbon nanotubes, because of their unique properties, such as high specific surface area and remarkable electronic and mechanical properties, are attractive materials for electrochemical energy storage devices.[5−7] However, the specific capacitance of pristine carbon nanotubes (CNTs) is too low to use them in many devices, because they mainly possess double-layer capacitances.[8,9] So, many efforts have been focused on the research of electrochemical behavior of CNT/active electrode materials composites. Until now, two types of active materials have been identified as the most promising electrode materials for ECs: multivalent metal oxides[10−13] and electrically conducting polymers (ECPs).[14−18] Compared to multivalent metal oxides, ECPs possess higher electric conductivity and more redox behaviors.[19]

As a typical ECP, polyaniline (PANi) has great potential in electrochemical capacitor application, because of its low cost, good processability, environmental stability, and reversible control of electrical properties by both charge-transfer doping and protonation.[20,21] To date, the CNT/PANi composite materials have been well-studied. Sainz et al.[22] investigated the formation mechanism of multiwalled carbon nanotube (MWNT)/PANi composites via in situ chemical polymerization. They discovered that two phases of PANi were developed simultaneously during polymerization in the presence of MWNTs. One phase is a "free" crystalline emeraldine base (EB); the other is the PANi, which has a more-planar structure along the MWNTs. However, Feng et al.[23] suggested that MWNT/PANi samples were composed of polycrystalline parts and amorphous parts. Moreover, the polycrystalline parts were distributed near the surface of the MWNTs, and the amorphous parts were distributed far away from the surface of the MWNTs. Besides, the influence of composite ratio on the electrochemical capacitances was also studied by many researchers. Gupta et al.[24] reported a specific capacitance of 463 F/g for the electropolymerization of SWNT/PANi composites at 73 wt % PANi. Recently, Zhang et al.[25] obtained the highest specific capacitance—500 F/g—for MWNT/PANi composites that contained 0.8 wt % MWNT via in situ electrochemical polymerization.

There has been recent interest in flexible safe energy devices, based on supercapacitors and batteries, to meet the various requirements of modern gadgets.[26−28] The success of these applications will be dependent on the availability of electronic materials that have good flexibility as well as good electrochemical behavior. Some researchers have tried to prepare flexible and lightweight CNT/PANi composite electrodes for use in supercapacitors. Liu et al.[29] constructed flexible sheets of CNT/PANi composites supercapacitors by painting a sheet of flexible plastic electrolyte with a composite material made of PANi and CNTs. Meng et al.[30] successfully prepared paperlike CNT/PANi composites via in situ chemical polymerization using a CNT network as a template. They also applied these paperlike CNT/PANi composites to prepare supercapacitors in series to light a red light-emitting diode (LED). However, more details about the electrochemical properties of such flexible CNT/PANi composites and the effect of electrode microstructure on their electrochemical behavior need to be learned to acquire optimum microstructure for superior capacitance. Electrochemical polymerization/degradation can sensitively adjust the morphology and microstructure of the PANi composites through flexible modulation of the electrolyte component and electric current.[31,32] In our previous work,[19] we prepared SWNT/PANi composite films on the SWNT/Ti electrode through an electrochemical polymerization/degradation process and improved the specific capacitance of composite by electrodegradation successfully. However, for free-standing SWNT/PANi composite films, the effects of electrodegradation processing on their microstructure and electrochemical behavior are seldom reported.

In this paper, the flexible SWNT/PANi composite films have been synthesized through in situ electrochemical polymerization/

* Authors to whom correspondence should be addressed. Tel.: +86 21 52412718. Fax: +86 21 52413122. E-mail addresses: liangao@mail.sic.ac.cn (L.G.), jingsun@mail.sic.ac.cn (J.S.).

10.1021/jp1092042
Published on Web 11/01/2010

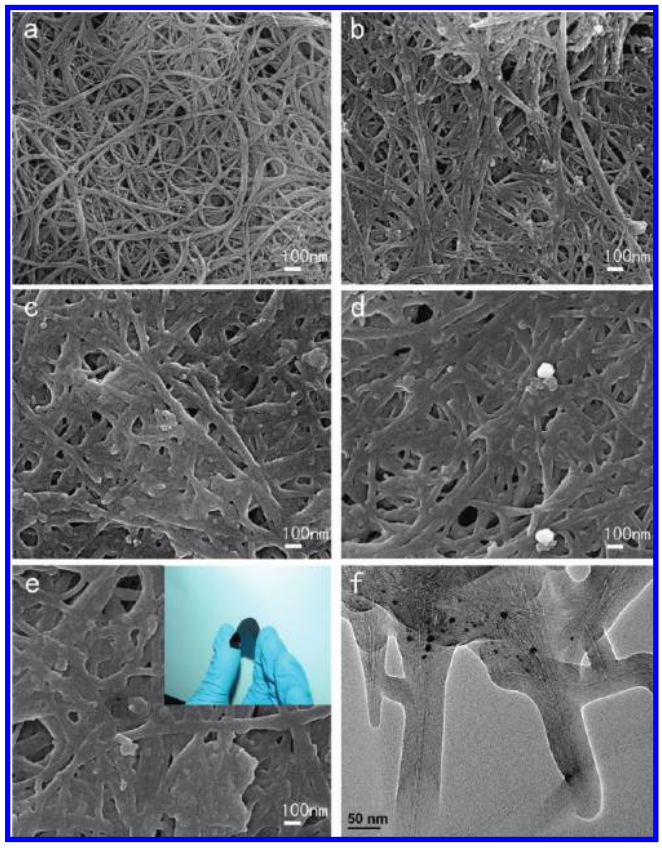

Figure 1. Scanning electron microscopy (SEM) images of (a) pure SWNT paper, as well as SWNT/PANi composite films ((b) SWNT/PANi50, (c) SWNT/PANi75, (d) SWNT/PANi90, (e) SWNT/PANi105) at the same magnification. Inset in panel (e) is a digital macrograph of the flexible composite film. (f) TEM image for SWNT/PANi90.

degradation process. By modulating the cycles of electropolymerization and electrodegradation, we successfully controlled the microstructure of SWNT/PANi composite films and attained the optimum microstructure for superior specific capacitance.

Experimental Section

Pristine SWNTs were synthesized by chemical vapor deposition at Chengdu Organic Institute, Chinese Academy of Sciences. The SWNTs were purified via the following process. First, 150 mg of pristine SWNTs were refluxed in 2.6 M nitric acid, at 140 °C for 24 h.[33] The solution then was filtered and washed by deionized water and absolute ethanol. Finally, the acid-SWNTs were dried at 60 °C for 24 h in a vacuum oven.

SWNT bucky paper was prepared in a typical process that has been reported in previous research.[34−36] Free-standing SWNT/PANi composite films were synthesized by a simple electrochemical method. In a three-electrode cell containing aqueous solution of 1 M H_2SO_4 + 0.05 M aniline, PANi was electrodeposited on the working electrode by potentiodynamic cycling between −0.2 V and 0.75 V (vs SCE) at a sweep rate of 20 mV/s. Here, SWNT bucky paper was attached to a thin nickel wire and used as the working electrode, while platinum wire and SCE were used as the counter and reference electrode, respectively. By controlling the electrodeposited cycles at 50, 75, 90, and 105, we obtained the composite electrodes SWNT/PANi50, SWNT/PANi75, SWNT/PANi90, and SWNT/PANi105, respectively. For comparison, pure PANi films were grown on a titanium plate under the same conditions. The SWNT/PANi90 electrodes then were electrodegraded in 1 M H_2SO_4 by potentiodynamic cycling between −0.5 V and 0.9 V (vs SCE) at a sweep rate of 10 mV/s. After 5, 10, 20, and 40 cycles of electrodegradation, we obtained samples that have been denoted as De5, De10, De20 and De40, respectively. Cyclic voltammetry (CV) measurements were performed in the voltage range from 0 V to 0.75 V (vs SCE) at a scan rate of 5 mV/s. The electrolyte was a 0.5 M H_2SO_4 aqueous solution. All the electrochemical experiments were performed using a Parstat 2273 electrochemical system (Princeton Applied Research Co, Ltd., USA).

The surface resistance of the SWNT/PANi composite films was measured by a standard four-probe in van der Pauw configuration, using an Accent HL5500 system at room temperature.

Field-emission scanning electron microscopy (FESEM) (Model JSM-6700F, JEOL, Tokyo, Japan), in addition to transmission electron microscopy (TEM) and high-resolution transmission electron microscopy (HRTEM) (Model 2100F, JEOL, Tokyo, Japan) were used to observe the morphology and microstructure of the composite electrodes. Raman spectra were obtained using

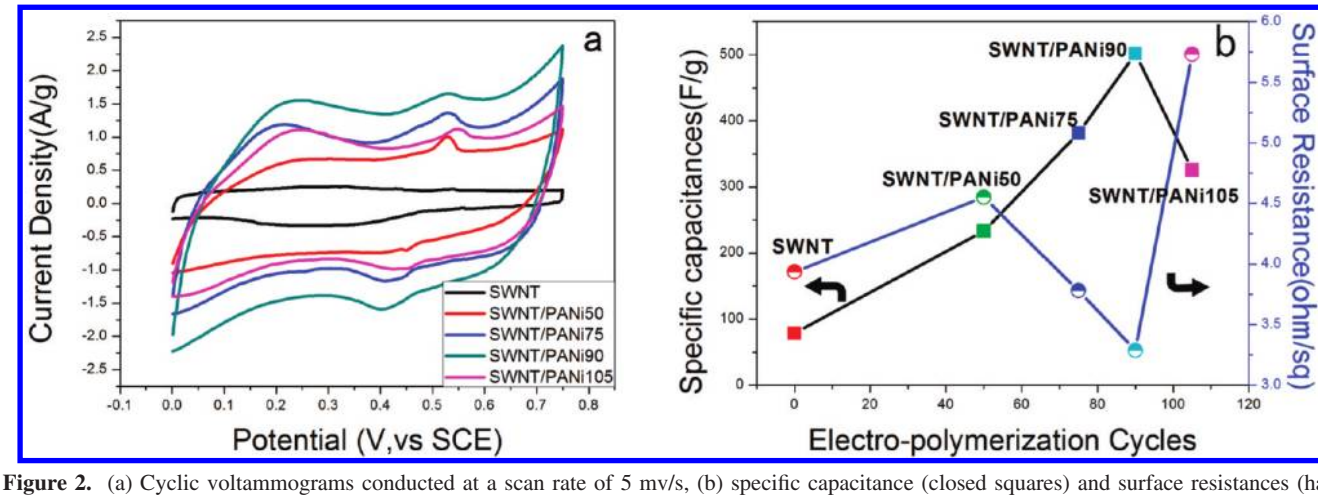

Figure 2. (a) Cyclic voltammograms conducted at a scan rate of 5 mv/s, (b) specific capacitance (closed squares) and surface resistances (half-filled circles) for pure SWNT paper and SWNT/PANi composite electrodes with electrochemical polymerization cycles at 50, 75, 90, and 105, respectively. (The arrows in panel (b) point to different *y*-axis labels.)

TABLE 1: Specific Capacitances and Surface Resistances of Pure SWNT Paper and Free-Standing SWNT/PANi Composite Films before and after Electrodegradation

Electrochemical Polymerization					
property	pure SWNT sheet	SWNT/PANi50	SWNT/PANi75	SWNT/PANi90	SWNT/PANi105
specific capacitance (F/g)	79	233.4	381.3	501.8	325.5
surface resistance (ohm/sq)	3.935	4.550	3.780	3.287	5.732

Electrochemical Degradation					
property	SWNT/PANi90	De5	De10	De20	De40
specific capacitance (F/g)	501.8	706.7	560	352	264
surface resistance (ohm/sq)	3.287	2.500	3.175	5.286	5.920

a Model LabRam-1B system (Jobin Yvon, France) under a radiation excitation wavelength of 632.8 nm.

Results and Discussion

Figure 1 displays typical SEM and TEM images of the SWNT/PANi composite films with different electropolymerization cycles. Macroscopically, the pristine SWNT sheet appeared very smooth. It was apparent that SWNT bundles randomly interwound together to form a three-dimensional (3D) SWNT network (see Figure 1a). The original CNT diameters were in the range of ~10−40 nm, whereas, for SWNT/PANi composite films, their diameters increased to ~50−110 nm after

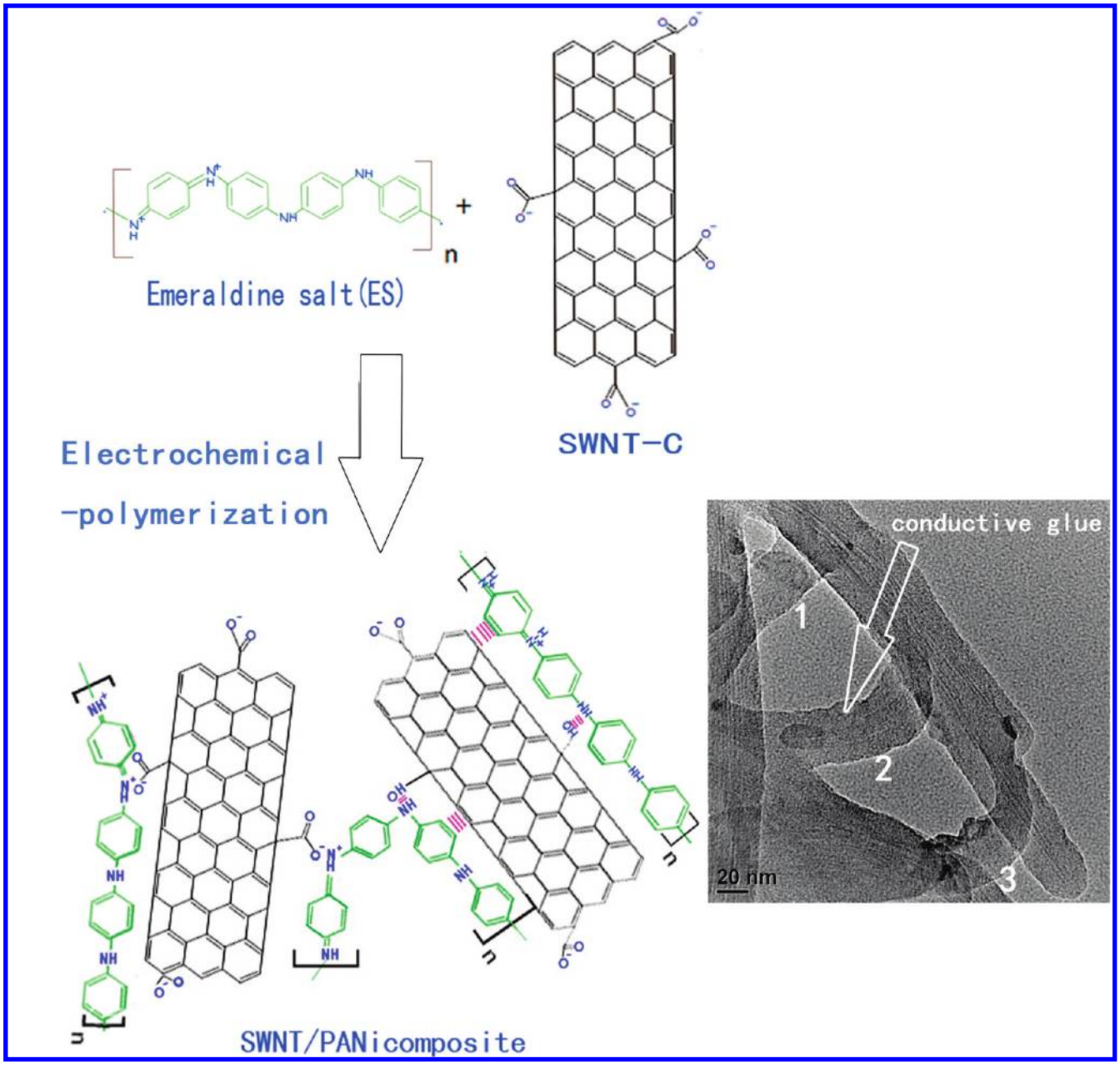

Figure 3. Schematic of the in situ electrochemical polymerization of the SWNT/PANi composite films. (Inset shows a TEM image of the "conductive glue".)

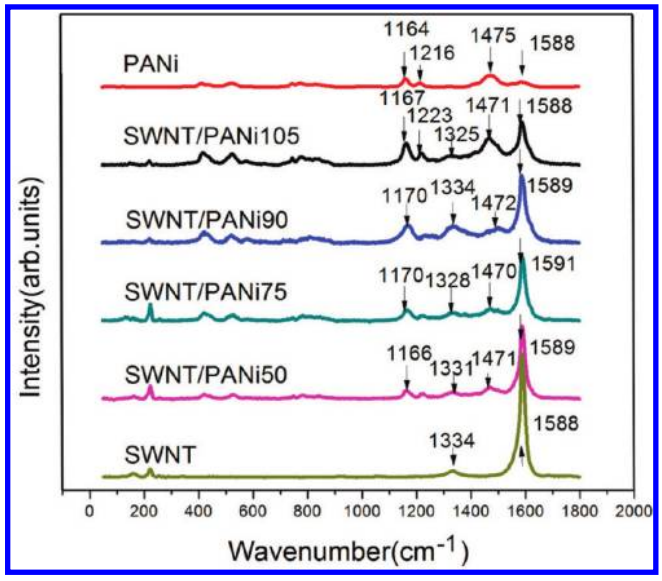

Figure 4. Raman spectra (λ_{exp} = 632.8 nm) for pure SWNT paper, pure PANi, and SWNT/PANi composite films with different electrochemical polymerization cycles (50, 75, 90, and 105, respectively).

electropolymerization. From Figure 1b to Figure 1e, the diameters of SWNT/PANi composites increased with prolongation of the electropolymerization process. In the case of SWNT/PANi50 (Figure 1b), there was only a small portion of the thin PANi layer that was coated on the surface of SWNTs sheets; however, for the SWNT/PANi75 and SWNT/PANi90 samples (see Figures 1c and 1d), it was apparent that their diameters were much larger than those of pristine SWNT sheet; meanwhile, the porous structure of SWNT network was retained. However, as the number of electropolymerization cycles increased to 105 (Figure 1e), there was excess PANi that not only filled into the pores, but also formed aggregates. The inset of Figure 1e indicates that, although a thick PANi layer coated on the surface of SWNT bucky paper was depicted, it still exhibited good flexibility. The paperlike SWNT/PANi films can be rolled up, bent, and even twisted without cracking, which is surely beneficial to its practical applications in some new areas. The TEM image in Figure 1f clearly demonstrated that the core−shell nanostructures of individual SWNT and SWNT bundles were coated with PANi.

Figure 2a compares the CV curves of SWNT/PANi composite films that had been synthesized in situ under different electropolymerization cycles. The CV curve of the pure SWNT bucky paper shows an almost-rectangular shape, which indicates that it mainly possesses electrical double-layer performance.[37] While the area of CV curves of the SWNT/PANi composite films is much larger than that of SWNT bucky paper, which suggests that the SWNT/PANi composite films show much better electrochemical behavior than that of SWNT bucky paper, because of their additional pseudo-capacitances and the charge-transfer complex formed among them.

Based on the CV results, the specific capacitance values of different samples are calculated according to eq 1:

$$C_m = \frac{1}{v(V_c - V_a)} \int_{V_a}^{V_c} I(V)\, dV \qquad (1)$$

where C_m is the specific capacitance, v is the potential scan rate (expressed in units of mV/s), the term $V_c - V_a$ represents

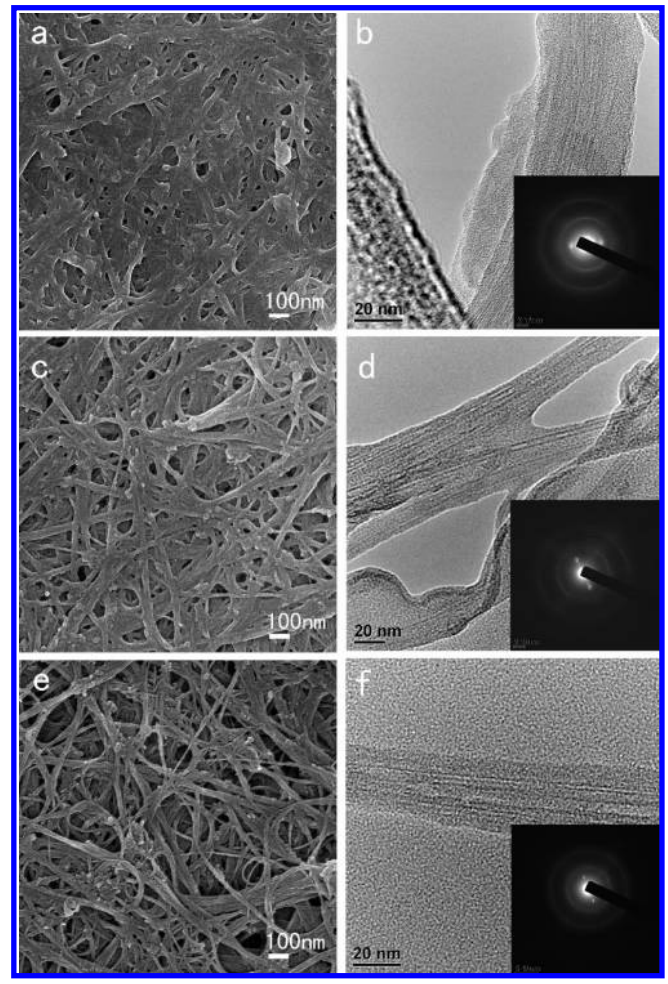

Figure 5. SEM and TEM images, and corresponding selected area electron diffraction (SAED) patterns, for SWNT/PANi90 (a, b) before electrochemical degradation, (c, d) after electrochemical degradation for 10 cycles, and (e, f) after electrochemical degradation for 40 cycles.

the sweep potential range, and $I(V)$ denotes the response current density (given in units of A/g).

According to the CV measurements, the specific capacitance of pure SWNT sheet is only 79 F/g, which is very similar to the result of Meng et al.[30] The specific capacitances of SWNT/PANi50, SWNT/PANi75, SWNT/PANi90, SWNT/PANi105 have been calculated to be 233.4, 381.3, 501.8, and 325.5 F/g, respectively (see Table 1). Their surface resistances, as measured by a standard four-probe method, also are shown in Table 1. This table shows that, when the number of electropolymerization cycles reached 90, we obtained the highest specific capacitance. However, when the number of cycles increased further to 105, the specific capacitance decreased to 325.5 F/g. The variations in electrochemical performances can be explained from the formation process of SWNT/PANi composite films. In the initial stage of the electropolymerization process, the π-bonded surface of the SWNTs interacted strongly with the conjugated structure of PANi, which facilitated the deposition of polymer chains on the surface of the SWNTs, forming a tubular coated layer. Here, the SWNT network served as a template for accelerating the nucleation and the growth of PANi. The strong $\pi-\pi$ interaction between flat PANi conformation and SWNTs, the additional possibility of charge transfer from planar polymer chain to SWNTs, and the increase in the active sites for faradaic reactions resulted in an increase in the specific capacitance.[25] However, as the polymerization continued, thicker PANi layers formed on the surface of SWNTs, causing weaker interaction between

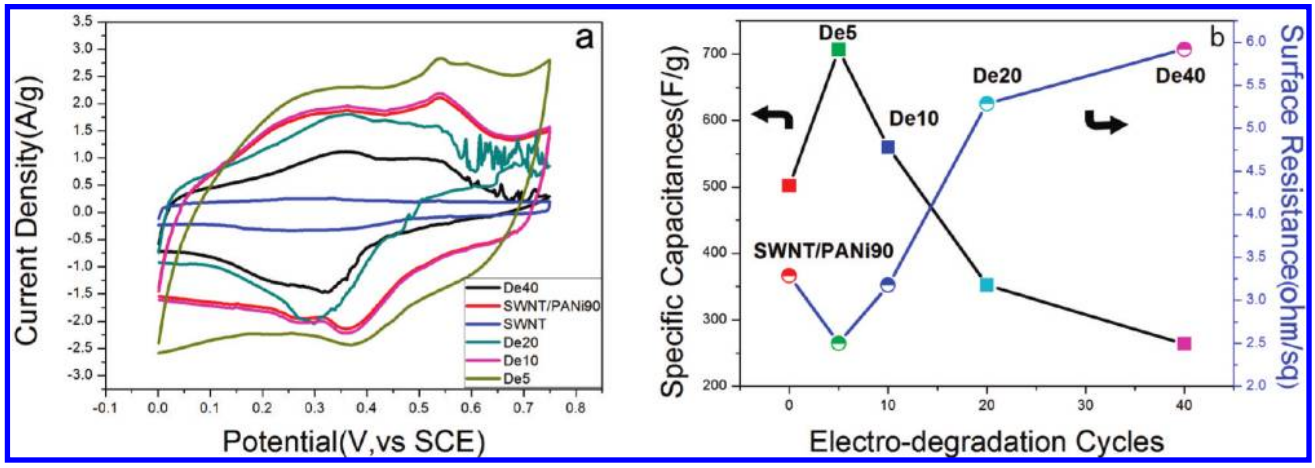

Figure 6. (a) Cyclic voltammograms conducted at a scan rate of 5 mv/s. (b) Specific capacitance (solid squares) and surface resistances (half-filled circles) for samples SWNT/PANi90 before and after electrochemical degradation for 5, 10, 20, 40 cycles. (The arrows in panel (b) point toward the different *y*-axis labels.)

the PANi and the SWNTs. Thus, some disordered PANi formed at off-lying spaces that surrounded the ordered polycrystalline regions.[19] On one hand, an increase in the thickness of the PANi impedes the ion diffusion and migration process; on the other hand, the appearance of disordered PANi makes the electrochemical reactions less reversible. Both of them result in a decrease in specific capacitance. These will be further verified by the changes in the surface resistance of SWNT/PANi composite films. From Figure 2b, the surface resistance showed an inverse tendency, compared to that of the specific capacitance of a SWNT/PANi composite. Combined with the SEM images for sample SWNT/PANi50, shown in Figure 1, only a small portion of PANi is distributed on the surface of the SWNT sheet. Less conductive pathways resulted in an increase in surface resistance.[38] Previous measurements have shown that the resistance of the SWNT network is dominated by the junctions between bundles.[39] One could expect that decreasing the intertube resistance could decrease the surface resistance in the network. Indeed, Ma et al.[40] reported that the contact resistances could be greatly decreased through in situ polymerization of a thin layer of self-doped conducting polymer (polyaniline boronic acid, PABA) around and along the CNTs. From SWNT/PANi50 to SWNT/PANi90, with more PANi polymerized on the surface of SWNT, the tube junction form of SWNT/SWNT has been replaced by SWNT/PANi/SWNT. PANi acts as a "conductive glue", effectively assembling the SWNTs into a conductive network, which results in a decrease in surface resistance. As shown in Figure 3, SWNT (core) well-coated with PANi (shell) interwound with each other to form a homogeneous conductive network. In the case of SWNT/PANi105, not only more excess PANi filled into pores in the films, but more disordered PANi were formed on the surface of SWNT/PANi composite films, which lead to an increase in surface resistance.

Figure 4 shows the Raman spectra of different SWNT/PANi composite films. The Raman spectrum of pure SWNT shows a strong peak at 1588 cm^{-1} and a weak peak at 1334 cm^{-1}, assigned to the G and D bands, respectively. For the pure PANi, C−H bending of the quinoid ring (1164 cm^{-1}), C═N stretching of the quinoid ring (1475 cm^{-1}), and C═C stretching of the quinoid ring (1588 cm^{-1}) were observed.[41,42] Note that the intensities of Raman peaks at 1170 and 1471 cm^{-1} in the composite films increase as the number of electropolymerization cycles increases. The increase in intensity of a characteristic peak of PANi indicated that more and more PANi was deposited onto the working electrode. Meanwhile, a remarkable decrease in the intensity of the band located at 1471 cm^{-1}, with respect to that of the band located at 1170 cm^{-1}, can be noticed from samples SWNT/PANi50 to SWNT/PANi90. This pronounced decrease gave evidence that a site-selective interaction between the quinoid ring of the doped polymer and the nanotubes occurred, as a consequence of the in situ polymerization.[43] The charge-transfer reaction between the polymer and charged SWNTs is similar to a doping process. The positive charges induced on the polymer chain were compensated by the anion-charged carboxyl-group-functionalized SWNT.[44] Thus, pernigraniline produced during electrochemical polymerization was readily reduced to the emeraldine state by the carboxyl group on the side of SWNTs (Figure 3). This interaction facilitates change-transfer processes between the components of the system and therefore influences the transport properties of the composites.[43] The surface resistance measurement (shown in Table 1) coincides with our analysis very well. However, when the number of electropolymerization cycles increased further up to 105, the I_{1471}/I_{1170} ratio increases again, which suggests that the interaction between the polymer and charged SWNTs becomes much weaker because of the increase in the thickness of the PANi layer. Thus, a more-disordered PANi was likely to be formed. The decrease in its surface resistance further verified this phenomenon. Based on the understanding above, we speculate that the specific capacitances of SWNT/PANi composite films could be improved further by controlling their microstructure.

Figure 5 shows SEM and TEM images, as well as corresponding selected area electron diffraction (SAED) patterns of samples SWNT/PANi90, De10, and De40. After electrodegradation, more pores formed on the surface of the SWNT/PANi composite films, and the thickness of the PANi layer packed on the surface of SWNTs decreased as the number of electrodegradation cycles increased. For sample De40, most of the PANi was electrodegraded and only a small amount of PANi remained on the surface of the SWNT films. The diffraction pattern in Figure 5b, corresponding to the free-standing SWNT/PANi90 film, shows distinct amorphous rings. As the number of electrodegradation cycles increased, the diffraction patterns show much weaker amorphous rings (shown in Figures 5d and 5f). These changes in diffraction patterns not only give evidence that amorphous PANi lay on the off-lying of SWNT/PANi90 composites, but also suggested that they could be dissolved by the electrodegradation reaction.

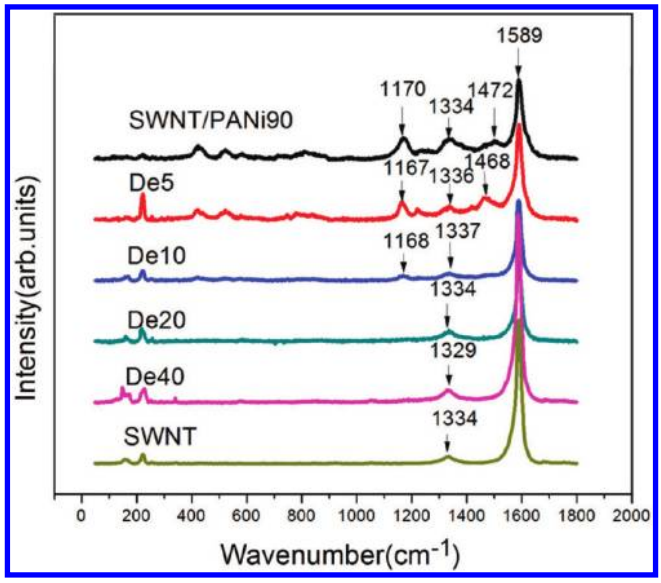

Figure 7. Raman spectra ($\lambda_{exp} = 632.8$ nm) for pure SWNT paper, as well as for SWNT/PANi90 before and after electrochemical degradation for 5, 10, 20, and 40 cycles.

Figure 6 exhibits the CV curves of SWNT/PANi90 before and after electrodegradation. According to the CV measurements, the highest specific capacitance of 706.7 F/g is obtained for sample De5, which is much larger than that of SWNT/PANi90; the specific capacitance of De10 is 560 F/g, which represents an increase of ~12%, relative to that of SWNT/PANi90. However, the specific capacitances of samples De20 and De40 are only 352 and 264 F/g, respectively (see Table 1). These results coincide well with their surface resistance, which showed an inverse tendency, compared to that of the specific capacitance (see Figure 6b). These unique relations suggest that low surface resistance is beneficial to the transfer of charged ions, thus improving the electrochemical behavior.

Similarly, during the electrodegradation process, off-lying disordered PANi was first dissolved to form ionic channels, because of their weaker interaction with SWNTs, and then unveiled polycrystalline regions became more available for electrochemical reaction. Later, the off-lying polycrystalline PANi was dissolved gradually as the electrodegradation reaction continued. The decrease in the mass of polycrystalline PANi resulted in weak pseudo-capacitance behavior from the Faradaic redox process, as well as the weak "conductive glue" effect, which impeded the ion diffusion and migration processes. It is because of these reasons that the specific capacitances for De20 and De40 become inferior to that of SWNT/PANi90.

The Raman spectra of different samples after electrodegradation further verified the changes in nanostructure during the electrodegradation process. As shown in Figure 7, increasing the number of electrodegradation cycles from 5 to 40 leads to almost-undetectable PANi signals in the Raman spectra, which suggests that electrodegradation is a gradual process and most of the off-lying PANi were dissolved when the number of electrodegradation cycles reached 40. For samples De20 and De40, characteristic peaks of PANi at 1170 and 1471 cm^{-1} were too weak to be detected. These results suggest that the nanostructure of SWNT/PANi composite films could be adjusted by electrochemical degradation, which provides a convenient way to assemble free-standing nanometer-sized SWNT/PANi films in a controlled manner.

Conclusion

In this study, the free-standing single-walled nanotube/polyaniline (SWNT/PANi) composite films have been successfully synthesized through an in situ electrochemical polymerization/degradation process. Structural analysis showed that the SWNT/PANi composite films had a SWNT (core)-doped PANi (shell) tubular structure with diameters of several tens to hundreds of nanometers, depending on the number of cycles of in situ electrochemical polymerization/degradation. Moreover, high-resolution transmission electron microscopy (HRTEM) and corresponding electronic diffraction pattern results show that polycrystalline and disordered PANi coexist in the SWNT (core)-doped PANi (shell) tubular structure, and off-lying PANi could be dissolved by electrochemical degradation. In addition to their well flexibility, SWNT/PANi composite films also show better electrochemical performance. The highest specific capacitance of 501.8 F/g was obtained for SWNT/PANi90. By controlling the number of electrodegradation cycles at 5, the specific capacitance was successfully enhanced to 706.7 F/g, which was attributed to dissolution of the off-lying disordered PANi and an increase in the number of available polycrystalline PANi regions. In conclusion, flexible SWNT/PANi composite films with controllable microstructures can be easily acquired via electrochemical polymerization/degradation processes and they have great promising applications in flexible electrochemical capacitors.

Acknowledgment. This work is supported by the National Science Foundation of China (No. 50972153).

References and Notes

(1) Otero, T. F.; Cantero, I. *J. Power Sources* **1999**, *81*, 838–841.
(2) Kotz, R.; Carlen, M. *Electrochim. Acta* **2000**, *45*, 2483–2498.
(3) Conway, B. E. *J. Electrochem. Soc.* **1991**, *138*, 1539–1548.
(4) Portet, C.; Taberna, P. L.; Simon, P. *Electrochim. Acta* **2005**, *50*, 4174–4181.
(5) Niu, C. M.; Sichel, E. K.; Hoch, R.; Moy, D.; Tennent, H. *Appl. Phys. Lett.* **1997**, *70*, 1480–1482.
(6) Coleman, J. N.; Khan, A. U.; Gun, Y. K. *Adv. Mater.* **2006**, *18*, 689–706.
(7) Chen, Z.; Appenzeller, J.; Lin, Y. M.; Sippel, O. J.; Rinzler, A. G. *Science* **2006**, *311*, 1735.
(8) Baughman, R. H.; Cui, C. X. *Science* **1999**, *284*, 1340–1344.
(9) Barisci, J. N.; Wallace, G. G.; Baughman, R. H. *J. Electrochem. Soc.* **2000**, *147*, 4580–4583.
(10) Hu, C. C.; Chang, K. H. *Electrochim. Acta* **2000**, *45*, 2685–2696.
(11) Yuan, A. B.; Zhang, Q. L. *Electrochem. Commun.* **2006**, *8*, 1173–1178.
(12) Ye, J. S.; Cui, H. F.; Liu, X.; Lim, T. M. *Small* **2005**, *1*, 560–565.
(13) Zheng, J. P.; Cygan, P. J.; Jow, T. R. *J. Electrochem. Soc.* **1995**, *142*, 2699–2703.
(14) Frackowiak, E.; Khomenko, V.; Jurewicz, K.; Lota, K.; Beguin, F. *J. Power Sources* **2006**, *153*, 413–418.
(15) Bozlar, M.; Miomandre, F.; Bai, J. B. *Carbon* **2009**, *47*, 80–84.
(16) Wei, D.; Kvarnstrom, C.; Lindfors, T.; Ivaska, A. *Electrochem. Commun.* **2007**, *9*, 206–210.
(17) Gupta, V.; Miura, N. *Electrochim. Acta* **2006**, *52*, 1721–1726.
(18) Chen, L.; Yuan, C. Z.; Dou, H.; Gao, B.; Chen, S. Y.; Zhang, X. G. *Electrochim. Acta* **2009**, *54*, 2335–2341.
(19) Xie, X. F.; Gao, L.; Sun, J.; Liu, Y. Q. *Carbon* **2008**, *46*, 1145–1151.
(20) Zhou, Y. K.; He, B. L.; Zhou, W. J.; Huang, J. E.; Li, X. H.; Wu, B.; Li, H. L. *Electrochim. Acta* **2004**, *49*, 257–262.
(21) Ghosh, P.; Chakrabarti, A.; Siddhanta, S. K. *Eur. Polym. J.* **1999**, *35*, 803–813.
(22) Sainz, R.; Benito, A. M.; Martinez, M. T. *Adv. Mater.* **2005**, *17*, 278–281.
(23) Feng, W.; Bai, X. D.; Lian, Y. Q.; Liang, J. *Carbon* **2003**, *41*, 1551–1557.
(24) Gupta, V.; Miura, N. *J. Power Sources* **2006**, *157*, 616–620.
(25) Zhang, J.; Kong, L. B.; Wang, B.; Luo, Y. C. *Synth. Met.* **2009**, *159*, 260–266.

(26) Pushparaj, V. L. *Proc. Natl. Acad. Sci. U.S.A.* **2007**, *104*, 13574–13577.
(27) Cui, L.-F.; Hu, L.; Choi, J. W.; Cui, Y. *ACS Nano* **2010**, *4*, 3671–3678.
(28) Lu, X. M.; Xia, Y. N. *Nat. Nanotechnol.* **2006**, *1*, 163–164.
(29) Liu, Q. *J. Power Sources* **2010**, *195*, 7480–7483.
(30) Meng, C. Z.; Liu, C. H.; Fan, S. S. *Electrochem. Commun.* **2009**, *11*, 186–189.
(31) Hu, C. C.; Chu, C. H. *Mater. Chem. Phys.* **2000**, *65*, 329–338.
(32) Wang, Z.; Yuan, J.; Li, M. *J. Electroanal. Chem.* **2007**, *599*, 121–126.
(33) Wang, Y.; Gao, L.; Sun, J.; Liu, Y. Q. *Chem. Phys. Lett.* **2006**, *432*, 205–208.
(34) Gou, J. H. *Polym. Int.* **2006**, *55*, 1283–1288.
(35) Wang, Z.; Liang, Z. Y.; Wang, B. *Composites, Part A* **2004**, *35*, 1225–1232.
(36) Smajda, R.; Kukovecz, A.; Konya, Z. *Carbon* **2007**, *45*, 1176–1184.
(37) Oh, J.; Kozlov, M. E. *Synth. Met.* **2008**, *158*, 638–641.
(38) Meng, C. Z.; Liu, C. H.; Fan, S. S. *Adv. Mater.* **2009**, *21*, 1–5.
(39) Stadermann, M.; Papadakis, S. J.; Falvo, M. R. *Phys. Rev. B* **2004**, 69.
(40) Ma, Y. F.; Cheung, W.; Wei, D. G.; Bogozi, A.; Chiu, P. L.; Wang, L.; Pontoriero, F.; Mendelsohn, R.; He, H. *ACS Nano* **2008**, *2*, 1197–1204.
(41) Cochet, M.; Louarn, G.; Quillard, S.; Buisson, J. P.; Lefrant, S. *J. Raman Spectrosc.* **2000**, *31*, 1041–1049.
(42) Quillard, S.; Louarn, G.; Lefrant, S. *Phys. Rev. B* **1994**, *50*, 12496–12508.
(43) Cochet, M.; Maser, W. K.; Benito, A. M. *Chem. Commun.* **2001**, 1450–1451.
(44) Baibarac, M.; Baltog, I.; Godon, C.; Lefrant, S.; Chauvet, O. *Carbon* **2004**, *42*, 3143–3152.

JP1092042